

PHYSICS

QC
166

J683

Journal of Vacuum Science & Technology A

JVST A

Second Series
Volume 12, Number 4, Part I
July/August 1994

PHYSICS-ASTRONOMY

27 1994

Vacuum, Surfaces, and Films

Papers from the
40th National Symposium of the
American Vacuum Society, Part I

Part I
History
Electronic Materials
Plasma Science
Thin Film
Vacuum Metallurgy
Vacuum Technology



An official journal of the American Vacuum Society
Published for the Society by the American Institute of Physics

JOURNAL
OF
VACUUM
SCIENCE &
TECHNOLOGY

A.
VACUUM,
SURFACES,
AND
FILMS

SER. 2

12
895-2604
1994

QC
166
J683
ser. 2
v.12
no.4

Journal of Vacuum Science & Technology A

Vacuum, Surfaces, and Films

JVST A

ISSN: 0734-2101
CODEN: JVTAD6

Editor: G. Lucovsky,
Department of Physics, North Carolina State University,
Raleigh, NC 27695-8202. Telephone: (919) 515-3468

Supervisor Editorial Office: Rebecca York,
Editorial Assistant: Marge Rodberg,
Journal of Vacuum Science and Technology, Microelectronics Center of North Carolina,
3021 Cornwallis Rd., Caller Box 13994, Research Triangle Park, NC 27709-3994.
Telephone: (919) 248-1861; FAX: 919-248-1857; E-mail: jvst@mcnc.org

Associate Editors:

Eric Kay, Critical Reviews and Special Issues
L. Brillson (95) Xerox Webster Research Center
J. A. Panitz (94) Sandia National Laboratories
C. J. Powell (95) National Inst. of Standards

W. D. Sproul (94) BIRL (Northwestern University)
John H. Thomas III (96) 3M Center
John T. Yates, Jr. (96) University of Pittsburgh

JVST Editorial Board:

S. M. Rosznagel, Chairman of Publications
Committee, IBM Watson Research Ctr.
A. A. Bright (95) IBM Watson Research Ctr.
S. Chambers (96) Pacific Northwest Laboratory
R. J. Colton (96) Naval Research Lab.
G. J. Exarhos (94) Pacific Northwest Laboratory
J. L. Freeouf (94) IBM Watson Research Lab.
U. J. Gibson (95) Dartmouth College

Dennis Manos, Assistant Chairman of Publications
Committee, College of William and Mary
T. M. Mayer (94) Sandia National Laboratory
B. S. Meyerson (96) IBM Watson Research Ctr.
Neil Peacock (95) HPS Division of MKS
Instruments, Inc.
D. Ruzic (96) University of Illinois

JVST Editorial Staff at AIP: Editorial Supervisor: Deborah McHone; Journal Coordinator: Elizabeth Belmont; Chief Production Editor: Margaret Reilly; Senior Production Editor: Adrienne Haddad

The **Journal of Vacuum Science and Technology A** is published six times annually (Jan/Feb, Mar/Apr, May/Jun, Jul/Aug, Sep/Oct, Nov/Dec) by the American Institute of Physics (AIP) for and under the editorial management of the American Vacuum Society (AVS). It is an official publication of the AVS and is received by all members of the Society. It is devoted to reports of original research, review articles, and Critical Review articles. The JVST A will include topics such as applied surface science, electronic materials and processing, fusion technology, plasma technology, surface science, thin films, vacuum metallurgy, and vacuum technology. It will contain the program and papers from the AVS National Symposium as well as the papers from other conferences and symposia sponsored by the AVS and its Divisions.

Submit Manuscripts to the Editorial Office of the *Journal of Vacuum Science and Technology*, Microelectronics Center of North Carolina, 3021 Cornwallis Rd., Caller Box 13994, Research Triangle Park, North Carolina 27709-3994. Manuscripts of papers present at AVS-sponsored conferences and symposia and being submitted to JVST A should be sent to the Guest Editor appointed for that particular conference. Before preparing a manuscript, authors should read "Information for Contributors," printed in the first issue of each volume of the journal. Submission of a manuscript is a representation that the manuscript has not been published previously nor currently submitted for publication elsewhere. Upon receipt of a manuscript the Editor will send the author a Transfer of Copyright Agreement form. This must be completed by the author and returned *only* to the Editorial Office prior to publication of an accepted paper in the *Journal of Vacuum Science and Technology A*. This written transfer of copyright, which previously was assumed to be implicit in the act of submitting a manuscript, is necessary under the 1978 copyright law in order for the AVS and AIP to continue disseminating research results as widely as possible. Further information may be obtained from AIP.

Publication Charge: To support the cost of wide dissemination of research results through publication of journal pages and production of a data base of articles, the author's institution is requested to pay a *page charge* of \$85 per page (with a one-page minimum). The charge (if honored) entitles the author to 100 free reprints. For Errata the minimum page charge is \$10, with no free reprints.

AIP's Physics Auxiliary Publication Service (PAPS) is a low-cost depository for material that is part of and supplementary to a published paper, but is too long to be included in the journal. Inquire of the Editor.

Advertising Rates will be supplied on request from AIP's Advertising Division [Telephone: (516) 576-2478]. Orders, advertising copy, and offset negatives should be sent to that division.

Copyright 1994, American Vacuum Society. Individual teachers, students, researchers, and libraries acting for them, are permitted to make copies of articles in this journal for their own use in research or teaching, including multiple copies for classroom or library reserve use, provided such copies are not sold. Copying for sale is subject to payment of copying fees. (See "Copying Fees" paragraph elsewhere in this journal.) Permission is granted to quote from this journal with the customary acknowledgment of the source. To reprint a figure, table, or other excerpt requires in addition the consent of one of the original authors and notification to AIP. Reproduction for advertising or promotional purposes, or republication in any form, is permitted only under license from AIP, which will normally require that the permission of one of the authors also be obtained. Direct inquiries to Office of Rights and Permissions, American Institute of Physics, 500 Sunnyside Blvd., Woodbury, NY 11797-2999.

American Vacuum Society

Officers

John R. Noonan, *President*
Argonne National Laboratory

John Weaver, *President-Elect*
University of Minnesota

William D. Westwood, *Secretary*
Bell-Northern Research Ltd.

N. Rey Whetten, *Treasurer/*
Technical Director
American Vacuum Society

H. Frederick Dylla, *Past-President*
Continuous Electron Beam
Accelerator Facility

Directors

Bruce Sartwell
Naval Research Laboratory

James Solomon
University of Dayton

Patricia Thiel
Iowa State University

Roger L. Stockbauer
Louisiana State University

Eric M. Stuve
University of Washington

Christine B. Whitman
CVC Products, Inc.

JVST

G. Lucovsky, *Editor-in-Chief*
N. Carolina State University

AVS Membership Information may be obtained from

Angela Mulligan
*AVS Membership
and Scholarship Secretary*
120 Wall Street
32nd Floor
New York, NY 10005
(212) 248-0200

Journal of
Vacuum Science
& Technology A

Vacuum, Surfaces, and Films

JVST A

Second Series
Volume 12, Number 4,
Part I
Jul/Aug 1994

Table of Contents for the Topical Conference on a Key to Competitiveness: The Science and Technology of Manufacturing A34

Table of Contents for the Topical Conference on Biomaterial Interfaces..... A38

PAPERS FROM THE 40TH NATIONAL SYMPOSIUM OF THE AMERICAN VACUUM SOCIETY

PART I

Preface..... A43

History

The American Vacuum Society and the people who have guided its development

Jack H. Singleton..... 895

Throughput-type pumps and ultrahigh vacuum

M. H. Hablanian..... 897

History of ultrahigh vacuum pressure measurements

P. A. Redhead 904

(Continued)

Journal of Vacuum Science & Technology A (ISSN: 0734-2101) is published six times annually (Jan/Feb, Mar/Apr, May/Jun, Jul/Aug, Sep/Oct, Nov/Dec) for the American Vacuum Society by the American Institute of Physics, 500 Sunnyside Blvd., Woodbury, NY 11797-2999. Membership in the American Vacuum Society includes \$17.50 from membership dues to be applied towards a subscription to *Journal of Vacuum Science & Technology A*.

Known office of publication is Thorofare, NJ. Second class postage paid at Thorofare, NJ and at additional mailing offices. POSTMASTER: Send address changes to *Journal of Vacuum Science & Technology A*, SLACK Inc., 6900 Grove Road, Thorofare, NJ 08086.

Subscription Prices (1994)

| | U.S.A. and Poss. | Can., Mex., Central & S. America & Caribbean | Europe, Asia, Africa & Oceania* |
|---------------------------|------------------------|---|------------------------------------|
| JVST A [†] | \$530 | \$555 | \$574 |
| JVST A [‡] | \$630 | \$655 | \$674 |
| JVST A and B [†] | \$630 | \$680 | \$718 |
| JVST A and B [§] | \$630 | \$655 | \$655 |
| JVST A and B [‡] | \$730 | \$780 | \$818 |

[†]Paper only.

[‡]Paper and CD-ROM.

[§]CD-ROM only.

*Nonmember subscriptions include air-freight service.

Back-number Prices: Single copy \$70; multipart issues \$70 per part.

Subscriptions, renewals, and address changes should be addressed to *Subscription Fulfillment Division, SLACK, Inc., 6900 Grove Road, Thorofare, NJ 08086*. Allow at least six weeks advance notice. For address changes please send both old and new addresses, and, if possible, include a label from the plastic mailing wrapper of a recent issue. For your convenience a **change-of-address form is included in every issue of *Physics Today*; please use it.**

AIP will honor a request for a missing journal issue only within six months of that issue's actual date of publication. Requests received for missing issues beyond six months of the actual publication date will not be honored. The issue may, however, be purchased at the single-copy price. (Subscription Fulfillment offices are located at SLACK Inc., 6900 Grove Road, Thorofare, NJ 08086.)

Single-copy orders (current and back issues) should be addressed to American Institute of Physics, Circulation and Fulfillment Division, 500 Sunnyside Blvd., Woodbury, NY 11797-2999.

Document Delivery: For information on obtaining copies of individual articles, contact AIP Circulation and Fulfillment Division, 500 Sunnyside Blvd., Woodbury, NY 11797-2999; phone: (516) 576-2277; (800) 344-6908; fax: (516) 394-9704; E-mail: elecprod@pinet.aip.org.

Copying fees: The code that appears on the first page of articles in this journal gives the fee for each copy of the article made beyond the free copying permitted by AIP. (See statement under "Copyright" elsewhere in this journal.) If no code appears, no fee applies. The fee for pre-1978 articles is \$0.25 per copy. With the exception of copying for advertising and promotional purposes, the express permission of AIP is not required provided the fee is paid through the *Copyright Clearance Center, Inc. (CCC), 27 Congress Street, Salem, MA 01970*. Contact the CCC for information on how to report copying and remit payment.

Microfilm subscriptions of complete volumes of the *Journal of Vacuum Science and Technology A* are available on 16 mm and 35 mm. The journal also appears in Sec. I of *Current Physics Microform (CPM)* along with 32 other journals published by the American Institute of Physics and its member societies. A *Microfilm Catalog* is available on request. The *Journal of Vacuum Science and Technology A* is indexed quarterly in *Current Physics Index*, a subject and author index (with abstracts) to all journals published by AIP and its member societies.

| | |
|---|-----|
| Some important developments in capture pumping technology in the last 40 years | |
| Kimo M. Welch | 915 |
| Ultrahigh vacuum in the semiconductor industry | |
| John F. O'Hanlon | 921 |
| Historical perspective of oriented and epitaxial thin films | |
| M. H. Francombe | 928 |
| History and current status of vacuum metallurgy | |
| Rointan F. Bunshah | 936 |
| Ultrahigh vacuum and surface science | |
| Paul W. Palmberg | 946 |
| Perspective on stresses in magnetron-sputtered thin films | |
| D. W. Hoffman | 953 |
| Development of ultrahigh vacuum technology for particle accelerators and magnetic fusion devices | |
| H. F. Dylla | 962 |

Electronic Materials

Chemical Routes to Group IV Epitaxy

| | |
|---|-----|
| Ultrahigh vacuum/chemical vapor deposition epitaxy of silicon and germanium-silicon heterostructures | |
| D. W. Greve, R. Misra, R. Strong, and T. E. Schlesinger | 979 |
| Silicon shot gas epitaxy: Dose-controlled digital epitaxy | |
| K.-J. Kim, M. Suemitsu, and N. Miyamoto | 986 |
| Heteroepitaxial growth of Si on GaP and GaAs surfaces by remote, plasma enhanced chemical vapor deposition | |
| S. Habermehl, N. Dietz, Z. Lu, K. J. Bachmann, and G. Lucovsky | 990 |

Strain and Defect Generation in Semiconductor Epitaxy

| | |
|--|------|
| III-V on dissimilar substrates: Epitaxy and alternatives | |
| J. De Boeck, P. Demeester, and G. Borghs | 995 |
| Molecular beam epitaxy grown III-V strain relaxed buffer layers and superlattices characterized by atomic force microscopy | |
| A. J. Howard, I. J. Fritz, T. J. Drummond, J. A. Olsen, B. E. Hammons, S. R. Kurtz, and T. M. Brennan | 1003 |
| Fabrication of relaxed $\text{Si}_{1-x}\text{Ge}_x$ layers on Si substrates by rapid thermal chemical vapor deposition | |
| D. Dutartre, P. Warren, F. Provenier, F. Chollet, and A. Péro | 1009 |
| Strain compensated heterostructures in the $\text{Si}_{1-x-y}\text{Ge}_x\text{C}_y$ ternary system | |
| J. L. Regolini, S. Bodnar, J. C. Oberlin, F. Ferrieu, M. Gauneau, B. Lambert, and P. Boucaud | 1015 |

Chemical Vapor Deposition of Metals and Insulators

| | |
|---|------|
| Low-Knudsen-number transport and deposition | |
| Hung Liao and Timothy S. Cale | 1020 |
| Comparison of boranol and silanol reactivities in boron-doped SiO_2 chemical vapor deposition from trimethyl borate and tetraethyl orthosilicate | |
| M. E. Bartram and H. K. Moffat | 1027 |
| W nucleation on TiN from WF_6 and SiH_4 | |
| S. L. Lantz, A. E. Bell, W. K. Ford, and D. Danielson | 1032 |

Electronic Structure and Optical Properties of Semiconductor Surfaces and Heterostructures

| | |
|--|------|
| Large oscillator strength of spatially indirect electron-hole recombination at type II heterojunctions: The InAlAs/InP case | |
| D. Bimberg, J. Böhrer, and A. Krost | 1039 |
| Ultraviolet photosulfidation of III-V compound semiconductors for electronic passivation | |
| Kevin R. Zavadii, Carol I. H. Ashby, Arnold J. Howard, and B. E. Hammons | 1045 |
| Strain relaxation induced deep levels in $\text{In}_{1-x}\text{Ga}_x\text{As}$ thin films | |
| A. Raisanen, L. J. Brillson, R. S. Goldman, K. L. Kavanagh, and H. H. Wieder | 1050 |

(Continued)

| | |
|---|------|
| Amorphous Si:B films: Microstructure and electrical properties | |
| G.-R. Yang, S. R. Soss, T. C. Nason, X.-F. Ma, A. Coccoziello, B. Y. Tong, Y. T. Zhu, J. Du, and K. F. Tjew | 1054 |
| Electrochemical sulfur passivation of visible (~670 nm) AlGaInP lasers | |
| A. J. Howard, C. I. H. Ashby, J. A. Lott, R. P. Schneider, and R. F. Corless | 1063 |
| Characterization of diamondlike carbon films grown by super-wide electron-cyclotron resonance plasma assisted chemical vapor deposition | |
| A. Ishii, S. Amadatsu, S. Minomo, M. Taniguchi, M. Sugiyu, and T. Kobayashi | 1068 |
| Transport and phototransport properties of plasma-deposited hydrogenated amorphous silicon nitrogen alloys, a-Si_{1-x}N_xH | |
| M. J. Williams, S. S. He, S. M. Cho, and G. Lucovsky | 1072 |
| Preliminary soft x-ray studies of β-SiC | |
| M. L. Shek, K. E. Miyano, Q.-Y. Dong, T. A. Callcott, and D. L. Ederer | 1079 |
| Monte Carlo simulation and measurement of silicon reactive ion etching profiles | |
| R. N. Tait, S. K. Dew, T. Smy, and M. J. Brett | 1085 |
| Investigation on the effect of isoelectronic substitution in ZnS_{1-x}Se_x alloys | |
| Art J. Nelson | 1090 |
| Structural characterization of GaN and GaAs_xN_{1-x} grown by electron cyclotron resonance-metalorganic molecular beam epitaxy | |
| S. Bharatan, K. S. Jones, C. R. Abernathy, S. J. Pearton, F. Ren, P. W. Wisk, and J. R. Lothian | 1094 |
| Posthydrogenation study of a-Si films grown by reactive magnetron sputtering | |
| Y. H. Liang and J. R. Abelson | 1099 |
| Sulfur passivation of Al_xGa_{1-x}As for ohmic contact formation | |
| Verlyn Fischer, E. Ristolainen, P. H. Holloway, W. V. Lampert, and T. W. Haas | 1103 |
| Kinetic and mechanistic study of the chemical vapor deposition of titanium dioxide thin films using tetrakis-(isopropoxo)-titanium(IV) | |
| Carl. P. Fictorie, John F. Evans, and Wayne L. Gladfelter | 1108 |
| Chemical states of the GaAs/Si interface | |
| Huijian Zhou and Wei Ho | 1114 |
| Be-doped GaAs layers grown at a high As/Ga ratio by molecular beam epitaxy | |
| D. H. Zhang, K. Radhakrishnan, S. F. Yoon, and H. M. Li | 1120 |
| Indium desorption from strained InGaAs/GaAs quantum wells grown by molecular beam epitaxy | |
| K. Radhakrishnan, S. F. Yoon, R. Gopalakrishnan, and K. L. Tan | 1124 |
| Effect of substrate temperature on dry etching of InP, GaAs, and AlGaAs in iodine- and bromine-based plasmas | |
| U. K. Chakrabarti, F. Ren, S. J. Pearton, and C. R. Abernathy | 1129 |
| Nanometer p-n junction formation and characterization | |
| W. M. Lau, L. J. Huang, W. H. Chang, I. Bello, T. Abraham, and M. King | 1134 |
| Growth and characterization of Si_{1-x}Ge_x/Si multilayers on patterned Si(001) substrates using gas source molecular beam epitaxy | |
| J. Zhang, A. Marinopoulou, J. Hartung, E. C. Lightowers, N. Anwar, G. Parry, M. H. Xie, S. M. Mokler, X. D. Wu, and B. A. Joyce | 1139 |
| Si 1s x-ray absorption spectra of epitaxial Si-Ge atomic layer superlattice and alloy films | |
| A. P. Hitchcock, T. Tylliszczak, M. L. M. Rocco, J. T. Francis, S. G. Urquhart, X. H. Feng, Z. H. Lu, J.-M. Baribeau, and T. E. Jackman | 1142 |
| Comparison of two epitaxial formation mechanisms in the SiGe system and the subsequent defect generation | |
| S. M. Prokes and A. K. Rai | 1148 |

Insulators of Semiconductors

| | |
|--|------|
| Optical anisotropy of singular and vicinal Si-SiO₂ interfaces and H-terminated Si surfaces | |
| T. Yasuda, D. E. Aspnes, D. R. Lee, C. H. Bjorkman, and G. Lucovsky | 1152 |
| CaF₂ overlayers to preserve the ideal termination of Sb/GaAs(110) | |
| A. M. Green, W. E. Spicer, C. Kim, R. Cao, and P. Pianetta | 1158 |

(Continued)

| | |
|---|------|
| GaAs formation by reduction of As₂O₃ and Ga₂O₃ at SiO₂/GaAs oxides/GaAs interfaces | |
| I. Jiménez, M. Moreno, J. A. Martín-Gago, M. C. Asensio, and J. L. Sacedón | 1170 |
| <i>Group III-V Epitaxial Growth and Transport</i> | |
| Real-time scanning microprobe reflection high-energy electron diffraction observations of III-V growth during molecular-beam epitaxy | |
| T. Isu, Y. Morishita, S. Goto, Y. Nomura, and Y. Katayama | 1176 |
| As capture and the growth of ultrathin InAs layers on InP | |
| D. E. Aspnes, M. C. Tamargo, M. J. S. P. Brasil, R. E. Nahory, and S. A. Schwarz | 1180 |
| Comparison of intrinsic and extrinsic carbon doping sources for GaAs and AlGaAs grown by metalorganic molecular beam epitaxy | |
| C. R. Abernathy, S. J. Pearton, F. Ren, W. S. Hobson, and P. W. Wisk | 1186 |
| Fundamental research and device applications of molecular beam epitaxy grown heterostructures | |
| C. Weisbuch | 1191 |
| Study of the epitaxial growth of GaAs(110) films by molecular beam epitaxy | |
| P. N. Fawcett, J. H. Neave, J. Zhang, and B. A. Joyce | 1201 |
| Plasma Science | |
| <i>Plasma Etching</i> | |
| Microloading effect prevention in SiO₂ contact-hole etching | |
| Shin-ichi Kato, Masaaki Sato, and Yoshinobu Arita | 1204 |
| Short-gas-residence-time electron cyclotron resonance plasma etching | |
| Kazunori Tsujimoto, Takao Kumihashi, Naoyuki Kofuji, and Shin'ichi Tachi | 1209 |
| <i>Modeling of Radio-Frequency and Microwave Plasma Sources</i> | |
| Modeling the electromagnetic excitation of a microwave cavity plasma reactor | |
| W. Tan and T. A. Grotjohn | 1216 |
| Modeling an inductively coupled plasma source | |
| A. P. Paranjpe | 1221 |
| Modeling and simulation of glow discharge plasma reactors | |
| Dimitris P. Lymberopoulos and Demetre J. Economou | 1229 |
| <i>Plasma Science and Technology I</i> | |
| Oxygen-plasma-enhanced crystallization of a-Si:H films on glass | |
| Aiguo Yin and S. J. Fonash | 1237 |
| Super-wide electron cyclotron resonance plasma source excited by traveling microwave as an efficient tool for diamondlike carbon film deposition | |
| A. Ishii, S. Amadatsu, S. Minomo, M. Taniguchi, M. Sugiyo, Y. Sakaguchi, and T. Kobayashi | 1241 |
| Investigation of thick, low-temperature plasma deposited silica films for waveguide fabrication | |
| M. Tabasky, E. S. Bulat, B. Tweed, and C. Herrick | 1244 |
| Examination of hydrogen etched mercury cadmium telluride by spectroscopic ellipsometry | |
| Glennis J. Orloff and Patricia B. Smith | 1252 |
| Reactive ion etching of copper with BCl₃ and SiCl₄: Plasma diagnostics and patterning | |
| B. J. Howard and Ch. Steinbrüchel | 1259 |
| Tapered aluminum interconnect etch | |
| Lynn R. Allen and Rick Rickard | 1265 |
| Operation of DIII-D with all-graphite walls | |
| K. L. Holtrop, G. L. Jackson, A. G. Kellman, R. L. Lee, and M. A. Hollerbach | 1269 |
| Production and characterization of doped mandrels for inertial-confinement fusion experiments | |
| R. Cook, G. E. Overturf III, S. R. Buckley, and R. McEachern | 1275 |
| <i>High-Density Plasma Processing I</i> | |
| Electron cyclotron resonance plasma source for conductive film deposition | |
| Toshiro Ono, Hiroshi Nishimura, Masaru Shimada, and Seitaro Matsuo | 1281 |

(Continued)

| | |
|---|------|
| Fluorocarbon high density plasmas. VIII. Study of the ion flux composition at the substrate in electron cyclotron resonance etching processes using fluorocarbon gases | |
| Karen H. R. Kirmse, Amy E. Wendt, Gottlieb S. Oehrlein, and Ying Zhang | 1287 |
| <i>Inertial Confinement Fusion Target Fabrication</i> | |
| Cryogenic targets and related technologies at ILE Osaka University | |
| T. Norimatsu, C. M. Chen, K. Nakajima, M. Takagi, Y. Izawa, T. Yamanaka, and S. Nakai | 1293 |
| Laser fusion target shell wall thickness from interference fringe shape analysis | |
| R. B. Stephens and M. D. Wittman | 1302 |
| <i>High-Density Plasma Processing II</i> | |
| Electron cyclotron resonance plasma and thermal oxidation mechanisms of germanium | |
| Y. Wang, Y. Z. Hu, and E. A. Irene | 1309 |
| <i>In situ</i> electron cyclotron resonance plasma surface cleaning of silicon | |
| Y. Z. Hu, P. P. Buaud, L. Spanos, Y. Q. Wang, M. Li, and E. A. Irene | 1315 |
| Helicon wave plasma reactor employing single-loop antenna | |
| Nobuhiro Jiwari, Takayuki Fukasawa, Hiroshi Kawakami, Haruo Shindo, and Yasuhiro Horiike | 1322 |
| Etching of aluminum alloys in the transformer-coupled plasma etcher | |
| Yunju Ra, Stephen G. Bradley, and Ching-Hwa Chen | 1328 |
| <i>Plasma Induced Damage</i> | |
| Damage to thin gate oxide during lightly doped drain spacer oxide etching | |
| Calvin T. Gabriel and Milind G. Weling | 1334 |
| Thin-oxide degradation along feature edges during reactive ion etching of polysilicon gates | |
| K. Markus, C. M. Osburn, P. Magill, and S. M. Bobbio | 1339 |
| Characterization of etch-induced damage for Si etched in Cl₂ plasma generated by an electron cyclotron resonance source | |
| K. T. Sung and S. W. Pang | 1346 |
| Investigation of plasma etch induced damage in compound semiconductor devices | |
| R. J. Shul, M. L. Lovejoy, D. L. Hetherington, D. J. Rieger, G. A. Vawter, J. F. Klem, and M. R. Melloch | 1351 |
| Magnetron enhanced reactive ion etching of GaAs in CH₄/H₂/Ar: Surface damage study | |
| G. F. McLane, W. R. Buchwald, L. Casas, and M. W. Cole | 1356 |
| <i>Plasma Enhanced Deposition</i> | |
| Critical ion energy and ion flux in the growth of films by plasma-enhanced chemical-vapor deposition | |
| L. Martinu, J. E. Klemberg-Sapieha, O. M. Küttel, A. Raveh, and M. R. Wertheimer | 1360 |
| Carbon content of silicon oxide films deposited by room temperature plasma enhanced chemical vapor deposition of hexamethyldisiloxane and oxygen | |
| J. A. Theil, J. G. Brace, and R. W. Knoll | 1365 |
| Low-temperature plasma-assisted oxidation combined with <i>in situ</i> rapid thermal oxide deposition for stacked-gate Si-SiO₂ heterostructures: Integrated processing and device studies | |
| V. Misra, S. V. Hattangady, T. Yasuda, X-L Xu, B. Hornung, G. Lucovsky, and J. J. Wortman | 1371 |
| <i>Plasma Science and Technology II</i> | |
| Computer simulation of mass-selective plasma-source ion implantation | |
| J. L. Shohet, E. B. Wickesberg, and Mark J. Kushner | 1380 |
| Two-dimensional self-consistent fluid simulation of radio frequency inductive sources | |
| G. DiPeso, V. Vahedi, D. W. Hewett, and T. D. Rognlien | 1387 |
| Effects of particle clouds in a plasma etch system on silicon dioxide wafer contamination | |
| S. M. Collins, J. F. O'Hanlon, and R. N. Carlile | 1397 |
| Plasma impedance and microwave interferometric measurements of electron concentrations in dual-frequency powered sulfur hexafluoride plasmas | |
| V. C. Jaiprakash and B. E. Thompson | 1403 |
| <i>Plasma-Surface Interactions</i> | |
| Effects of ion-induced electron emission on magnetron plasma instabilities | |
| M. B. Hendricks, P. C. Smith, D. N. Ruzic, A. Leybovich, and J. E. Poole | 1408 |

(Continued)

| | |
|--|------|
| Role of ions in reactive ion etching | |
| J. W. Coburn..... | 1417 |
| Importance of the molecular identity of ion species in reactive ion etching at low energies | |
| I. Bello, W. H. Chang, and W. M. Lau..... | 1425 |
| <i>Plasma Processing-Particulate Formation/In Situ Ellipsometry</i> | |
| Real-time observation of ultrathin silicon oxide film growth using rapid ellipsometry | |
| H. Kuroki, K. G. Nakamura, I. Kamioka, T. Kawabe, and M. Kitajima..... | 1431 |
| Thin Film | |
| <i>Optical Films</i> | |
| Energetic particles in the sputtering of an indium-tin oxide target | |
| K. Tominaga, M. Chong, and Y. Shintani | 1435 |
| Optical thin films for waveguide applications | |
| Jose M. Mir and John A. Agostinelli..... | 1439 |
| Deposition of nonlinear optical films of potassium titanyl phosphate (KTiOPO₄) by pulsed excimer laser ablation | |
| Fulin Xiong, M. Hagerman, H. Zhou, V. Kozhevnikov, G. K. Wong, K. Poeppelmeier, J. B. Ketterson, R. P. H. Chang, and C. W. White..... | 1446 |
| <i>Energetic Condensation</i> | |
| Inert gases in sputtered tungsten: A test of predictive capability | |
| D. W. Hoffman, J.-S. Park, and T. S. Morley | 1451 |
| Estimations and results of energetic condensation processes in relation to hard carbon deposition | |
| B. Rother..... | 1457 |
| In situ measurement of thin-film conductivity during and after energetic condensation | |
| Michael Mausbach, Guido van Kronenberg, and Horst Ehrich..... | 1463 |
| Infrared absorption and nuclear magnetic resonance studies of carbon nitride thin films prepared by reactive magnetron sputtering | |
| Dong Li, Yip-Wah Chung, Shengtian Yang, Ming-Show Wong, Farshid Adibi, and William D. Sproul..... | 1470 |
| <i>Diamond Film Growth Processes</i> | |
| One-point numerical modeling of microwave plasma chemical vapor deposition diamond deposition reactors | |
| E. Hyman, K. Tsang, A. Drobot, B. Lane, J. Casey, and R. Post | 1474 |
| Properties of chemical vapor infiltration diamond deposited in a diamond powder matrix | |
| Janda K. G. Panitz, David R. Tallant, Charles R. Hills, and David J. Staley..... | 1480 |
| <i>Diamond and Diamondlike Carbon</i> | |
| Interfacial reactions of ion beam deposited a-C films on ZnS | |
| T. Bruce, L. J. Huang, I. Bello, W. M. Lau, P. Panchhi, V. Strnad, and M. High..... | 1487 |
| Deposition and characterization of nanocrystalline diamond films | |
| Dieter M. Gruen, Xianzheng Pan, Alan R. Krauss, Shengzhong Liu, Jianshu Luo, and Christopher M. Foster..... | 1491 |
| Auger electron spectroscopy of laser deposited a-C, a-C:H, microcrystalline diamond | |
| Peter Kovarik, E. B. D. Bourdon, and R. H. Prince | 1496 |
| <i>Aspects of Thin Films</i> | |
| Dependence of material properties of radio-frequency magnetron-sputtered, Cu-doped, ZnTe thin films on deposition conditions | |
| T. A. Gessert, X. Li, T. J. Coutts, A. R. Mason, and R. J. Matson..... | 1501 |
| Study of ion-beam-sputtered ZnO films as a function of deposition temperature | |
| Y. Qu, T. A. Gessert, T. J. Coutts, and R. Noufi | 1507 |
| Reaction layer formation and fracture at chemically vapor deposited diamond/metal interfaces | |
| Scott S. Perry and Gabor A. Somorjai..... | 1513 |
| Interface studies of the diamond film grown on the cobalt cemented tungsten carbide | |
| F.-M. Pan, J.-L. Chen, T. Chou, T.-S. Lin, and L. Chang..... | 1519 |

(Continued)

| | |
|--|------|
| Sputtering yield of optical materials: Sigmund's model and experimental results | |
| S. Scaglione, L. Caneve, and F. Sarto | 1523 |
| High temperature behavior of reactively sputtered AlN films on float glass substrates | |
| M. Arbab and J. J. Finley | 1528 |
| Raman spectroscopic study of the formation of $t\text{-MoSi}_2$ from Mo/Si multilayers | |
| M. Cai, D. D. Allred, and A. Reyes-Mena | 1535 |
| Preferential sputtering of silicon from metal silicides at elevated temperatures | |
| C. Hedlund, P. Carlsson, H.-O. Blom, S. Berg, and I. V. Katardjiev | 1542 |

Thin Film Characterization

| | |
|--|------|
| Accelerator based secondary-ion mass spectrometry for impurity analysis | |
| J. M. Anthony, J. F. Kirchhoff, D. K. Marble, S. N. Renfrow, Y. D. Kim, S. Matteson, and F. D. McDaniel | 1547 |
| Direct current sputter deposition of titanium nitride controlled <i>in situ</i> by soft x-ray emission spectroscopy | |
| P. B. Legrand, J. P. Dauchot, M. Hecq, M. Charbonnier, and M. Romand | 1551 |
| Studies of thin-film growth, adsorption, and oxidation by <i>in situ</i>, real-time, and <i>ex situ</i> ion beam analysis | |
| Yuping Lin, A. R. Krauss, O. Auciello, Y. Nishino, D. M. Gruen, R. P. H. Chang, and J. A. Schultz | 1557 |
| <i>In situ</i> x-ray reflectivity measurements of thin film structural evolution | |
| Eric Chason and Marc Chason | 1565 |

Vacuum Metallurgy

Diamond, CBN, and Other Ultrahard Coatings

| | |
|---|------|
| Effect of stoichiometry on the phases present in boron nitride thin films | |
| L. B. Hackenberger, L. J. Piloni, R. Messier, and G. P. Lamaze | 1569 |
| Deposition of diamondlike carbon using a planar radio frequency induction plasma | |
| D. L. Pappas and J. Hopwood | 1576 |
| Pull-test adhesion measurements of diamondlike carbon films on silicon carbide, silicon nitride, aluminum oxide, and zirconium oxide | |
| R. A. Erck, F. A. Nichols, and J. F. Dierks | 1583 |

Physical Vapor Deposition and Chemical Vapor Deposition Coating Applications

| | |
|---|------|
| Biased magnetron sputter deposition of corrosion resistant Al-Zn alloy thin films | |
| L. Li and W. B. Nowak | 1587 |
| Multilayer, multicomponent, and multiphase physical vapor deposition coatings for enhanced performance | |
| William D. Sproul | 1595 |
| (Ti_{1-x}Al_x)N coatings by plasma-enhanced chemical vapor deposition | |
| Sang-Hyeob Lee, Ho-Joon Ryoo, and Jung-Joong Lee | 1602 |

Plenary Session on Fundamental Processes of Polycrystalline Film Growth

| | |
|--|------|
| Microstructural study of sputter-deposited CdTe thin films | |
| X. Li, T. A. Gessert, R. J. Matson, J. F. Hall, and T. J. Coutts | 1608 |
| Influence of ion mass and ion energy on microstructure of ion assisted deposited zinc selenide thin films | |
| L. Caneve, S. Scaglione, D. Flori, and S. Martelli | 1614 |

Advances in Deposition Technologies and Novel Techniques

| | |
|---|------|
| Effects of target polycrystalline structure and surface gas coverage on magnetron <i>I-V</i> characteristics | |
| A. Leybovich, T. Kuniya, P. C. Smith, M. B. Hendricks, and D. N. Ruzic | 1618 |
| Multiple jets and moving substrates: Jet Vapor Deposition of multicomponent thin films | |
| B. L. Halpern and J. J. Schmitt | 1623 |
| Advanced electron beam source for ultrahigh vacuum (molecular beam epitaxy) and high vacuum applications of thin film deposition | |
| J. W. Moore and N. K. Tsujimoto | 1628 |

(Continued)

| | |
|--|------|
| Electron beam evaporator constructed from aluminum alloy and the gettering effect of chromium films | |
| S. Nakada, M. Yamaguchi, M. Yamamoto, and H. Ishimaru | 1631 |

Vacuum Technology

Large Vacuum Systems

| | |
|--|------|
| Vacuum system design of the International Thermonuclear Experimental Reactor pellet fueling system | |
| R. A. Langley, M. J. Gouge, and D. J. Santeler | 1635 |
| Construction and commissioning of the Synchrotron Radiation Research Center vacuum system | |
| G. Y. Hsiung, J. R. Huang, J. G. Shyy, D. J. Wang, J. R. Chen, and Y. C. Liu | 1639 |
| Vacuum characteristics of an oxygen-free high-conductivity copper duct at the KEK Photon Factory ring | |
| Y. Hori, M. Kobayashi, and Y. Takiyama | 1644 |
| Optimization of the configuration of the vacuum pumps in the KEK 2.5-GeV linac | |
| Y. Saito, K. Kakiyama, and G. Horikoshi | 1648 |
| Early vacuum systems and process descriptions used to deposit optical coatings | |
| C. Alexander | 1653 |

Vacuum Issues in Accelerators

| | |
|--|------|
| Cold beam tube photodesorption and related experiments for the Superconducting Super Collider Laboratory 20 TeV proton collider | |
| V. V. Anashin, G. Derevyankin, V. G. Dudnikov, O. B. Malyshev, V. N. Osipov, C. L. Foerster, F. M. Jacobsen, M. W. Ruckman, M. Strongin, R. Kersevan, I. L. Maslennikov, W. C. Turner, and W. A. Lanford | 1663 |
| Photon desorption measurements of copper and copper plated beam tubes for the SSCL 20 TeV proton collider | |
| C. L. Foerster, C. Lanni, I. Maslennikov, and W. Turner | 1673 |
| Proposed warm bore beam-pipe assemblies and associated vacuum systems for the worlds two largest particle detectors | |
| G. R. Chapman and J. X. Zhou | 1678 |

Pumps and Innovative Pumping Methods

| | |
|---|------|
| Detection of small pressure pulses in an ion pumped ultrahigh vacuum system | |
| G. Rupschus, R. Niepraschk, K. Jousten, and M. Kühne | 1686 |
| Comparison between several new molecular drag pumps and turbomolecular pumps | |
| Ji-guo Chu | 1690 |
| Turbomolecular pump with an ultimate pressure of 10^{-12} Torr | |
| Hajime Ishimaru and Hiromi Hisamatsu | 1695 |

Vacuum Materials

| | |
|--|------|
| Permeation of argon, carbon dioxide, helium, nitrogen, and oxygen through Mylar windows | |
| M. Mapes, H. C. Hseuh, and W. S. Jiang | 1699 |
| Sealing technique for aluminum to stainless steel CF flange pairs | |
| T. Ishigaki, K. Shibuya, H. Sakaue, and S. H. Be | 1705 |
| Evaluation of different cleaning techniques for oxygen-free high-conductivity copper | |
| Vijendran P. Rao and Michael P. Friedlander | 1709 |
| Comparison of photodesorption yields using synchrotron radiation of low critical energies for stainless steel, copper, and electrodeposited copper surfaces | |
| J. Gómez-Goñi, O. Gröbner, and A. G. Mathewson | 1714 |
| Vacuum outgassing of artificial dielectric ceramics | |
| Viet Nguyen-Tuong | 1719 |

Pressure and Flow Measurements A

| | |
|---|------|
| Performance of the cold cathode gauges in a high and misaligned magnetic field | |
| H. C. Hseuh, W. S. Jiang, and M. Mapes | 1722 |
| Development of a primary standard ultrahigh vacuum calibration station | |
| P. D. Levine and J. R. Sweda | 1727 |

(Continued)

| | |
|---|------|
| Pressure measurement by laser ionization: Direct counting of generated ions by imaging of their spatial distribution | |
| S. Ichimura, S. Sekine, K. Kokubun, and H. Shimizu..... | 1734 |
| Expanded-range, sealed parts leak testing technology for helium mass spectrometer leak detection | |
| D. G. Mahoney..... | 1740 |
| Gas-flow experiments in the transition region | |
| Donald J. Santeler..... | 1744 |
| <i>Water in Vacuum Systems, Outgassing and Cleaning</i> | |
| Outgassing behavior on aluminum surfaces: Water in vacuum systems | |
| J. R. Chen, J. R. Huang, G. Y. Hsiung, T. Y. Wu, and Y. C. Liu..... | 1750 |
| X-ray photoelectron spectroscopy analysis of aluminum and copper cleaning procedures for the Advanced Photon Source | |
| R. A. Rosenberg, M. W. McDowell, and J. R. Noonan..... | 1755 |
| Characteristics of extremely fast pump-down process in an aluminum ultrahigh vacuum system | |
| M. Miki, K. Itoh, N. Enomoto, and H. Ishimaru..... | 1760 |
| Study of cleaning agents for stainless steel for ultrahigh vacuum use | |
| J. D. Herbert, A. E. Groome, and R. J. Reid..... | 1767 |
| Model for water outgassing from metal surfaces. II | |
| Minxu Li and H. F. Dylla..... | 1772 |
| Analysis of offgassed water: Calibration and techniques | |
| James A. Basford..... | 1778 |
| CUMULATIVE AUTHOR INDEX | 1782 |

PART II

| | |
|--|-----------|
| Surface Science/Electronic Materials/Nanometer-Scale Science and Technology/Thin Film | |
| <i>Alloys and Bimetallic Epitaxy</i> | 1787-1799 |
| <i>Nucleation and Growth: Metals on Metals</i> | 1800-1824 |
| <i>Metal and Semiconductor Nucleation and Growth</i> | 1825-1847 |
| Electronic Materials/Surface Science | |
| <i>Semiconductor Surface Structure and Dynamics</i> | 1848-1857 |
| Electronic Materials/Surface Science/Nanometer-Scale Science and Technology | |
| <i>Semiconductor Surface Cleaning and Passivation</i> | 1858-1881 |
| Surface Science/Nanometer-Scale Science and Technology | |
| <i>Liquid-Solid Interfaces: Real and Model Systems</i> | 1882-1890 |
| Nanometer-Scale Science and Technology/Biomaterial Interfaces | |
| <i>Nanometer-Scale Biotechnology</i> | 1891-1903 |
| Electronic Materials/Thin Film | |
| <i>Metal-Semiconductor Interfaces</i> | 1904-1919 |
| Thin Film/Surface Science/Nanometer-Scale Science and Technology | |
| <i>Nucleation and Growth: Semiconductors on Semiconductors</i> | 1920-1937 |

(Continued)

Electronic Materials/Plasma Science

| | |
|---|-----------|
| <i>In Situ Diagnostics and Control of Growth and Deposition</i> | 1938-1956 |
| <i>Dry Etching for Micro- and Nanofabrication</i> | 1957-1991 |

Thin Film/Nanometer-Scale Science and Technology/Vacuum Technology

| | |
|--|-----------|
| <i>Sensors/Mechanical Properties of Thin Films</i> | 1992-2004 |
|--|-----------|

Nanometer-Scale Science and Technology/Surface Science/Electronic Materials/Applied Surface Science

| | |
|---|-----------|
| <i>Nanostructural Properties of Surfaces and Interfaces</i> | 2005-2028 |
|---|-----------|

Surface Science

| | |
|---|-----------|
| <i>Dynamics of Adsorption/Desorption</i> | 2029-2044 |
| <i>Novel Structures and Structural Techniques</i> | 2045-2062 |
| <i>Molecular Adsorption and Desorption</i> | 2063-2068 |
| <i>Aspects of Surface Science</i> | 2069-2169 |
| <i>Surface Reactions I</i> | 2170-2182 |
| <i>Surface Electronic Properties of Metals</i> | 2183-2204 |
| <i>Semiconductor Surface Cleaning and Passivation</i> | 2205-2214 |
| <i>Magnetic Films and Interfaces</i> | 2215-2223 |
| <i>Dynamics of Adsorbates and Reactions</i> | 2224-2234 |
| <i>Semiconductor Etching Reactions</i> | 2235-2239 |
| <i>Adsorbate Structure and Reactions</i> | 2240-2264 |
| <i>Semiconductor Surface Reactions</i> | 2265-2292 |
| <i>Dynamics of Nonthermal Surface Chemistry</i> | 2293-2297 |
| <i>Oxides and Oxidation</i> | 2298-2322 |
| <i>Semiconductor Structure: Surfaces and Interfaces</i> | 2323-2331 |

Applied Surface Science

| | |
|--|-----------|
| <i>Quantitative Analysis and Data Handling</i> | 2332-2356 |
| <i>Depth Profiling</i> | 2357-2377 |
| <i>Adhesion and Polymer-Metal Interfaces</i> | 2378-2397 |
| <i>Corrosion and Surface Modification</i> | 2398-2401 |
| <i>Aspects of Applied Surface Science</i> | 2402-2461 |
| <i>Applications of Synchrotron Radiation</i> | 2462-2477 |
| <i>Radiation and Beam Modifications of Surfaces</i> | 2478-2490 |
| <i>Polymer/Organic Surfaces and Interfaces</i> | 2491-2522 |
| <i>Self-Assembled Monolayers/Langmuir-Blodgett Films</i> | 2523-2536 |
| <i>Small Area Analysis</i> | 2537-2548 |

Nanometer-Scale Science and Technology

| | |
|--|-----------|
| <i>Nanotechnology I: Electro- and Mechanical Devices</i> | 2549-2564 |
| <i>Aspects of Nanometer Science and Technology</i> | 2565-2590 |
| <i>Innovations in Proximal Probes II</i> | 2591-2599 |

Kinetic and mechanistic study of the chemical vapor deposition of titanium dioxide thin films using tetrakis-(isopropoxo)-titanium(IV)

Carl. P. Fictorie, John F. Evans, and Wayne L. Gladfelter

Center for Interfacial Engineering and Department of Chemistry, University of Minnesota, Minneapolis, Minnesota 55455

(Received 4 October 1993; accepted 24 January 1994)

The mechanism of TiO_2 thin film deposition on single crystal TiO_2 by chemical vapor deposition (CVD) using tetrakis(isopropoxo)titanium(IV) (TTIP) has been investigated. The structure of the rutile(100) surface has been shown to form a 1×3 reconstruction using reflection high-energy electron diffraction. Temperature programmed reaction spectroscopy and molecular beam scattering have been employed to probe the kinetics of the reaction of TTIP and to identify reaction products. The deposition mechanism involves two parallel pathways to form TiO_2 : at lower temperatures (500–650 K) propene and isopropanol are formed as products; at higher temperatures (>650 K) propene and water are formed as products in a second pathway that becomes dominant. An activation energy of 57 ± 8 kJ/mol has been measured for the first pathway. The results for the single crystal surface are compared to earlier work on polycrystalline substrates.

I. INTRODUCTION

Titanium dioxide (TiO_2) has been proposed as a material for use as a dielectric insulator in metal oxide semiconductors (MOS) for a variety of applications including memory devices, dielectric filter stacks,^{1,2} and chemically resistant antireflective coatings for optical devices^{3,4} because of its high dielectric constant, its chemical stability, and its optical transparency in the visible and near infrared regions.

Particularly in the fabrication of microelectronic devices, the chemical vapor deposition (CVD) of TiO_2 is of interest to accommodate the decreasing size of features and ease of control over deposition conditions.^{2,5} However, the physical and chemical properties of the CVD precursors are infrequently related to the resultant properties of the deposited films such that full control over the deposition can be established.

The CVD of TiO_2 has been studied using a variety of precursors, focusing primarily on titanium tetrachloride (TiCl_4) plus water⁴ or titanium alkoxides [$\text{Ti}(\text{OR})_4$, where R =ethyl or isopropyl].^{1-3,5,6} Most widely reported are studies of the structure and properties of the deposited films, rather than the mechanistic chemistry of the deposition reactions.

In this paper, the relationship between the structure of the deposited TiO_2 film and the chemistry of the deposition process using tetrakis-(isopropoxo)-titanium(IV) (TTIP) as a precursor has been investigated. We have focused on epitaxial growth because of the influence of this chemistry on the formation of defects in the films which must be finely controlled in the fabrication of devices used in technological applications.^{7,8}

II. EXPERIMENT

The temperature programmed desorption (TPD), molecular beam scattering (MBS), and reflection high-energy electron diffraction (RHEED) experiments were performed in the two chamber ultrahigh vacuum (UHV) CVD/thin film characterization system illustrated in Fig. 1. The main chamber

(~ 60 L) was pumped by a 510 L/s (N_2) Balzers turbomolecular pump and a titanium sublimation pump. The chamber was arranged in three levels. The lowest level was equipped with a Physical Electronics Model 15-255G double pass cylindrical mirror analyzer (CMA) which was used for Auger electron spectroscopy (AES). The intermediate level was used for sample transfer between the two chambers. The upper level was equipped with a differentially pumped Extrel C50 quadrupole mass spectrometer (QMS) with a mass range of 2–750 amu, which was used for the TPD and MBS experiments. The QMS was separated from the main chamber by a skimmer with a 3 mm orifice in front of which the sample was placed for the TPD experiments. The QMS chamber (~ 7 L) was pumped by a 170 L/s (N_2) Balzers turbomolecular pump. The upper level also includes a Physical Electronics 04-303A 5 kV ion gun which was differentially pumped through the QMS chamber. Argon was used for all the sputtering. The main chamber had a base pressure of 2×10^{-10} Torr and an operating pressure of about 2×10^{-9} Torr. The QMS chamber had a base pressure of $\sim 1 \times 10^{-9}$ Torr.

The reactor chamber (~ 20 L) was pumped by a 170 L/s Balzers turbomolecular pump and a titanium sublimation pump. It was equipped with a Physical Electronics 06-190 electron gun (10 kV) used for RHEED experiments. The diffraction patterns were displayed on a phosphor screen located 20 ± 1 cm from the sample. The electron beam was focused onto the sample at an angle of 1.5° – 2° from the surface plane. Patterns were recorded using a Polaroid camera. Lattice constants were determined using GaAs(100) as a reference. The base pressure of this chamber was typically 1×10^{-9} Torr and could be operated as high as 1×10^{-5} Torr for CVD experiments.

The reactor and main chambers were connected via a 4 in. gate valve. The reactor was attached via a $2\frac{3}{4}$ in. gate valve to a six-way cross used for a load lock to allow for quick transfer of samples in and out of the UHV system. Transfer of samples into the reactor, and between the chambers, were made using magnetically coupled transfer rods. The sample

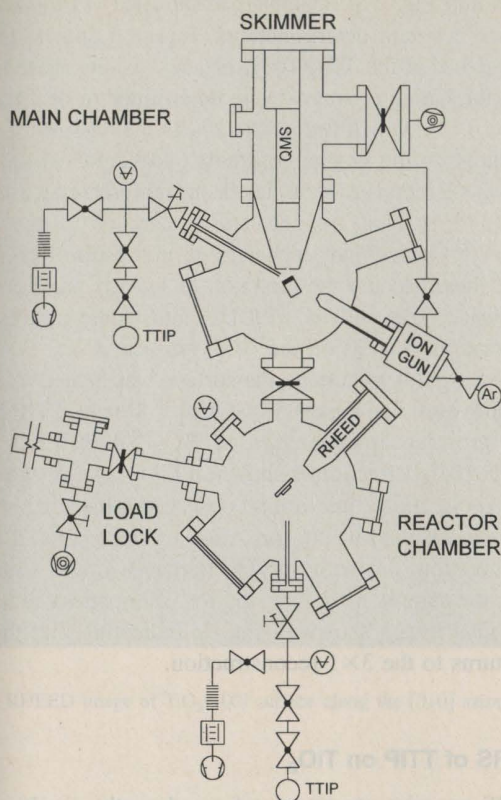


FIG. 1. Diagram of the CVD-TF system.

manipulators used in the system were capable of x , y , and z linear motions with z axis and azimuthal rotations.

Two types of sample mounts were used in the system. RHEED experiments were done by mounting the sample onto a molybdenum disk which was designed for use with the transfer system. The sample was held in place with a molybdenum clip using indium between the sample and disk as a thermal contact. These samples were heated from the back side of the disk via an electron beam heater. The sample temperature was monitored using an optical pyrometer which viewed the sample from outside the system. Temperatures in the range of 273–1073 K were attainable using this arrangement. However, increasing the temperature above 873 K resulted in the evaporation of indium from beneath the sample, with the resultant loss of thermal contact.

A second sample mount was used for the temperature programmed reaction spectroscopy (TPRS) and MBS experiments. It consisted of a U-shaped tantalum foil (0.23 mm thick) attached to a copper block which was in thermal contact with a liquid nitrogen reservoir. The sample was clamped to the tantalum foil with molybdenum clips and the temperature of the sample was measured using a chromel-alumel (K -type) thermocouple clamped between the molybdenum clip and the surface of the sample. The sample was radiatively heated from the back side using a tungsten filament powered by a manually controlled 120 V ac variable transformer. In this configuration temperatures in the range from 195 to 1073 K and heating rates of up to 20 K/s were possible. This mount was used only in the main chamber,

and did not allow for sample transfer between the two chambers. For TPD experiments, the sample was placed ~ 5 mm from the end of the doser (described below) for adsorption of the precursor onto the substrate. It was then moved to a position ~ 1 mm in front of the orifice of the skimmer for the temperature ramp. In the MBS experiments, the sample was located at the point where the center axes of the doser and QMS housing intersect; meanwhile, a constant flux of precursor was impinged on the substrate throughout the temperature ramp.

TiO₂ (rutile) single crystals (12 mm \times 12 mm \times 1 mm) in the (100) orientation (Commercial Crystal Laboratories) were used for the TPD, MBS, and RHEED experiments. It was found that reproducible TPD and MBS experiments on a given crystal could be achieved only after the procedure reported by Muryn *et al.*⁹ was performed. This involved sputtering the surface using 5 kV Ar⁺ for 20–30 min and then annealing at ~ 1100 K for 20 min in vacuum. This treatment changed the color of the crystal from a pale transparent yellow to an opaque metallic gray, consistent with the observations reported by Muryn *et al.*, in which they concluded that the presence of surface defects in the form of the 3×1 reconstruction has negligible effects on the reactivity of H₂O. The gray color is also consistent with the formation of crystallographic shear planes associated with the loss of small amounts of oxygen from the bulk.¹⁰

AES spectra were acquired using an electron energy of 3 kV in the counting mode [$N(E)$]. These spectra were then differentiated mathematically using the Savitsky–Golay differentiation algorithm. Mass spectra were taken using an electron energy of 30 eV to minimize fragmentation of the precursor. Both the CMA and the QMS were controlled by a Zenith 386 microcomputer. The CMA was interfaced via a Physical Electronics Model 137 adapter card and software which controls the CMA and provides some data manipulation capabilities. The QMS was interfaced using a Metrabyte DAS-HRES data acquisition board which controls the mass selection on the QMS and reads the analog output of the QMS as well as the thermocouple output from the sample using software written in house.

The dosers and gas manifolds used on the system were constructed of $\frac{1}{4}$ in. stainless steel VCR components. The manifold was pumped by an Alcatel 2020A rotary vane pump (26.9 m³/h) with a MDC molecular sieve trap. The precursor vessel was a glass bulb made from a glass to stainless steel transition attached to a stainless steel tube which connects to a Nupro valve which was used to isolate the tube. The pressure in the manifold was measured using a MKS Baratron capacitance manometer (Model 315B, 10 Torr range). The manifold was attached to the chamber via a Varian leak valve. The doser was a $\frac{1}{4}$ in. o.d. stainless steel tube. The precursor was outgassed by three freeze–pump–thaw cycles using ice water as the coolant. During TPD and MBS experiments the manifold (but not the precursor vessel) was heated to ~ 80 °C to prevent condensation of the precursor. The isolation valve was left open during dosing with the pressure in the manifold controlled by partially closing the valve between the manifold and the pump. The manifold



FIG. 2. RHEED image of the annealed TiO₂(100) surface along the [010] azimuth.

pressure was maintained between 15 and 20 mTorr by this method.

III. RESULTS AND DISCUSSION

A. RHEED of TiO₂(100)

RHEED photographs of the (100) surface are shown in Figs. 2 and 3. Figure 2 is the pattern attributed to the [010]



FIG. 3. RHEED image of the annealed TiO₂(100) surface along the [001] azimuth.

azimuth and Fig. 3 is attributed to the [001] azimuth based on lattice constant determinations. Figure 4 shows the surface structure of the TiO₂(100) surface.¹¹ Using these photographs, the lattice constants were determined to be 14.5 ± 0.5 Å \times 3.0 ± 0.1 Å, which is consistent with a 3×1 surface structure relative to the known constants (4.49 Å \times 2.96 Å).¹¹

This 3×1 reconstruction has been interpreted as a loss of every third row of oxygen atoms parallel to the [001] direction.^{9,12} It does not appear to be the result of crystallographic shear because the direction of shear is parallel to the (100) surface (the shift is $1/2\langle 011 \rangle$) and would not result in the formation of steps on the (100) surface.

Following this treatment, the surface was heated to 873 K in vacuum and then exposed to 1×10^{-6} Torr of TTIP for 15 min to grow an epitaxial film of TiO₂.⁷ A RHEED photo along the [010] direction is shown in Fig. 5. An image along the [001] direction could not be observed. This suggests that the growth resulted in the formation of steps parallel to the [001] direction, but with varying terrace widths.⁹ Upon annealing the sample as before, the RHEED pattern returns to the original image shown in Fig. 2, indicating that the surface returns to the 3×1 reconstruction.

B. TPRS of TTIP on TiO₂

TPRS experiments were performed on the single crystal TiO₂(100) surface using TTIP. In these experiments ~ 20 L was adsorbed onto the TiO₂ surface at about 343 K.¹³ Then the temperature of the sample was increased to about 973 K at a constant rate of 5 K/s. The results of this experiment are shown in Fig. 6.

The following ion fragments were monitored during the TPRS and MBS experiments: TTIP, $m/e=225$; propene, $m/e=39$; isopropanol, $m/e=45$; water, $m/e=18$; and acetone, $m/e=43$. The ion fragments used were selected because of minimal overlap of daughter ion masses which originate from different molecular species. Isopropanol was corrected for a contribution from TTIP and acetone was corrected for contributions from both isopropanol and TTIP.

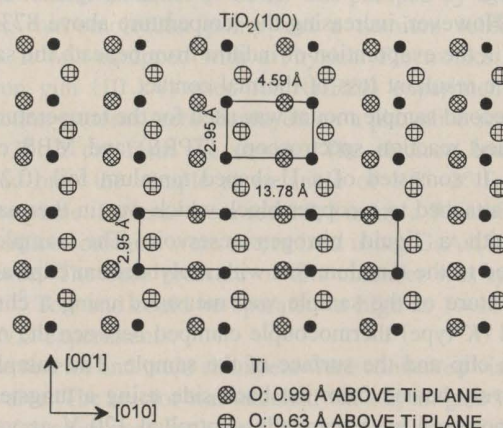


FIG. 4. Diagram of TiO₂(100) surface showing [010] and [001] azimuthal directions.

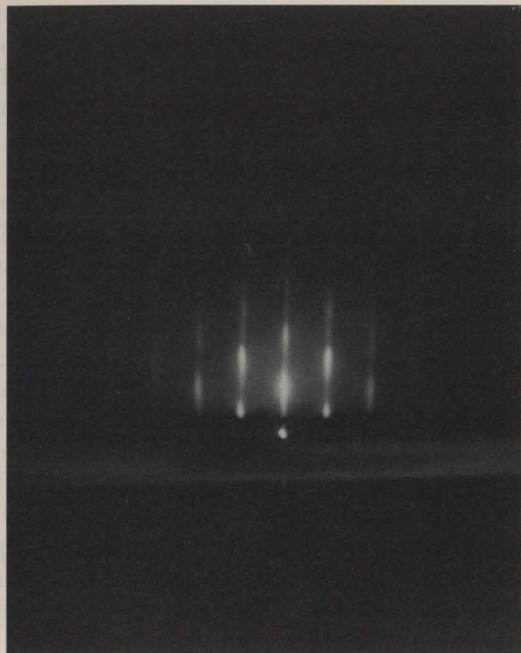


FIG. 5. RHEED image of TiO₂(100) surface along the [010] azimuth after CVD.

The data shows that no TTIP is desorbed under these conditions, indicating that the monolayer deposited at 343 K is adsorbed irreversibly. Propene and isopropanol are the only products observed in the TPRS experiment.

In control experiments using isopropanol as the adsorbate it was observed that isopropanol desorbs molecularly below

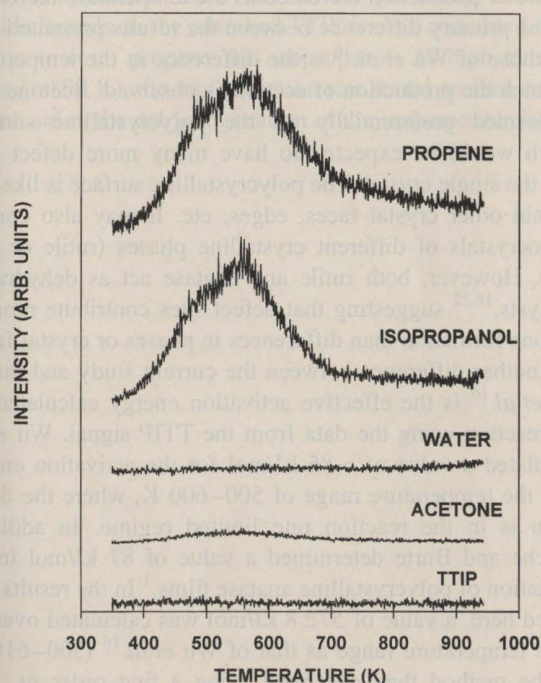


FIG. 6. TPRS spectrum of TTIP after a dose of 20 L and using a 5.3 K/s heating rate.

423 K. Propene would not adsorb onto the TiO₂ substrate at the lowest temperatures attempted here (193 K). Malet and Munuera¹⁴ performed TPD experiments with water on rutile powders and found that water will dissociatively adsorb to form surface hydroxyl groups, which desorb as water with a peak temperature of 590 K. In the TPRS experiment with TTIP, the desorption of propene and isopropanol are not the rate limiting steps, suggesting that one of the reaction steps is rate limiting. Also, propene and isopropanol peaks track each other closely, indicating that the rate limiting step forms both species simultaneously.

Using the first order kinetic model of Redhead,¹⁵ with an assumed preexponential value of 10^{12} and an experimental heating rate of 5.3 K/s, the activation energy is 134 ± 2 kJ/mol. This value is similar to that of Wu *et al.*¹⁶ (130–135 kJ/mol) and suggests that the rate limiting chemistry is similar in both cases.

C. MBS of TTIP on TiO₂(100)

MBS experiments were performed using TTIP on the single crystal TiO₂(100) surface. The experiment is performed by increasing the temperature of the sample from ~70 to ~600 °C at a constant rate of 2 K/s and then allowing the sample to cool with the radiative heater off, while maintaining a constant flux of precursor and monitoring the precursor and reaction products using the QMS.

The data for a flux of 1×10^{-6} Torr TTIP is shown in Fig. 7, showing signal for the precursor TTIP and the primary

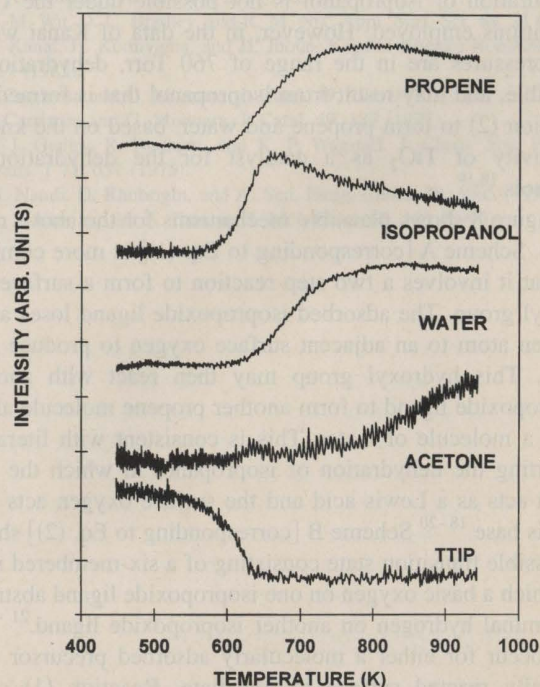
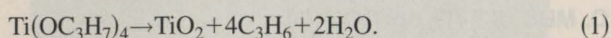


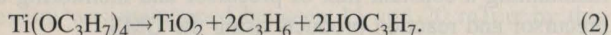
FIG. 7. MBS data for TTIP. The following fragments were monitored to give the resultant data: TTIP, $m/e=225$; propene, $m/e=39$; isopropanol, $m/e=45$ (corrected for contribution from TTIP); water, $m/e=18$; and acetone, $m/e=43$ (corrected for contributions from isopropanol and TTIP). These were chosen for the minimal mutual overlap. The data are shown for a TTIP pressure of 1×10^{-6} Torr.

products propene, isopropanol, water, and acetone. The rate of the reaction becomes significant above 530 K and all of the precursor is consumed by 640 K. The most striking feature is observed in the product profile for isopropanol. Here the signal intensity increases above 570 K, similar to propene, but reaches a maximum near 660 K, and then decreases at higher temperatures. In the profile for water, the signal intensity does not start to increase until the temperature rises above 610 K. Because these temperatures do not coincide, and because the TPRS data shows that water is not formed when isopropanol is generated, we conclude that there are different, parallel reaction pathways which generate isopropanol and propene separately from water and propene.

Kanai *et al.*¹⁷ reported a reaction stoichiometry for the formation of particles of TiO₂ in the gas phase using TTIP. They determined that the only products in addition to TiO₂ were propene and water from which they identified the following reaction:



This stoichiometry is consistent with our results in the higher temperature regime where little isopropanol is formed. It does not account for the production of isopropanol. The corresponding stoichiometry for the reaction of TTIP to form propene and isopropanol is



The conclusion of parallel reaction pathways requires the consideration of both of these reactions to form the observed products. These reactions must act independently because the dehydration of isopropanol is not possible under the UHV conditions employed. However, in the data of Kanai where the pressures are in the range of 760 Torr, dehydration is possible, and may result from isopropanol that is formed via reaction (2) to form propene and water, based on the known reactivity of TiO₂ as a catalyst for the dehydration of alcohols.^{18,19}

Figure 8 shows plausible mechanisms for the above reactions. Scheme A [corresponding to Eq. (1)] is more complex in that it involves a two step reaction to form a surface hydroxyl group. The adsorbed isopropoxide ligand loses a hydrogen atom to an adjacent surface oxygen to produce propene. This hydroxyl group may then react with another isopropoxide ligand to form another propene molecule along with a molecule of water. This is consistent with literature reporting the dehydration of isopropanol in which the titanium acts as a Lewis acid and the surface oxygen acts as a Lewis base.^{18–20} Scheme B [corresponding to Eq. (2)] shows a possible transition state consisting of a six-membered ring, in which a basic oxygen on one isopropoxide ligand abstracts a terminal hydrogen on another isopropoxide ligand.²¹ This can occur for either a molecularly adsorbed precursor or a partially reacted surface intermediate. Reaction (1) commences at a higher temperature than reaction (2) because the abstraction of hydrogen to the surface is less facile than the formation of the six-membered intermediate.

Wu *et al.*¹⁶ have done MBS experiments similar to those described above. They used a polycrystalline TiO₂ substrate prepared by CVD and observed the formation of acetone,

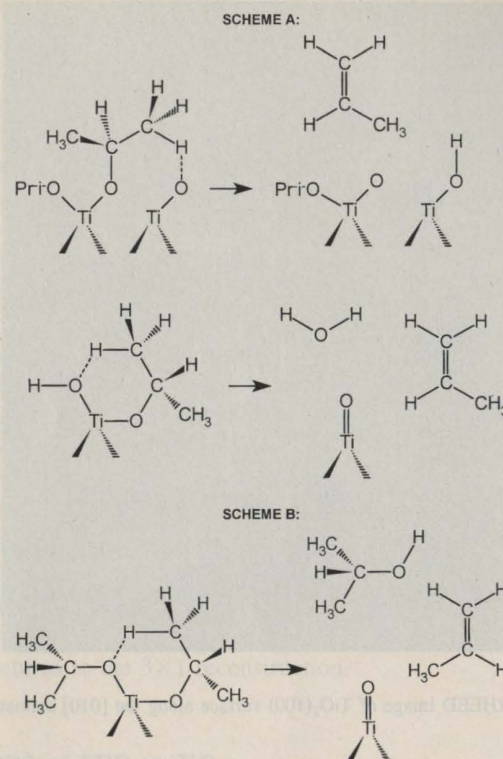


FIG. 8. Mechanistic schemes for reactions (1) and (2) in the CVD of TiO₂ using TTIP.

isopropanol, propene, and water over the temperature range of 500–800 K. They also noted the decrease of isopropanol and acetone signals above 650 K, while the rates of propene and water production increased as the temperature increased.

The primary difference between the results presented here and those of Wu *et al.*¹⁶ is the difference in the temperature at which the production of acetone is observed. Acetone may be formed preferentially on the polycrystalline surface, which would be expected to have many more defect sites than the single crystal. The polycrystalline surface is likely to contain other crystal faces, edges, etc. It may also contain microcrystals of different crystalline phases (rutile or anatase). However, both rutile and anatase act as dehydration catalysts,^{18,22} suggesting that defect sites contribute more to acetone formation than differences in phases or crystal faces.

Another difference between the current study and that of Wu *et al.*¹⁶ is the effective activation energy calculated for the reaction using the data from the TTIP signal. Wu *et al.* calculated a value of ~85 kJ/mol for the activation energy over the temperature range of 500–600 K, where the deposition is in the reaction rate limited regime. In addition, Rauche and Burte determined a value of 87 kJ/mol in the formation of polycrystalline anatase films.¹ In the results presented here, a value of 57 ± 8 kJ/mol was calculated over the same temperature range as that of Wu *et al.*¹⁶ (500–610 K) by the method they described using a first order fit. This difference in activation energies is due to the differences in surface structure, either from the defects of the polycrystalline surface or from the difference in surface structure be-

tween rutile and anatase. An analysis of the data using a second order equation gives a poorer fit to the data.

This value for the activation energy (57 ± 8 kJ/mol) is significantly different than the value determined from the TPRS data (134 ± 2 kJ/mol). If the TPRS data are analyzed using $E_a = 57 \pm 8$ kJ/mol, the preexponential factor is found to range from 4×10^3 to 2×10^5 s⁻¹. For comparison, Carrizosa and Munuera¹⁸ have performed TPRS experiments with isopropanol on anatase and measured an activation energy of 92 ± 2 kJ/mol and a preexponential factor of 4.7×10^6 s⁻¹ for the formation of propene. The two schemes shown in Fig. 8 are consistent with a low activation barrier deriving from the relatively stable six-membered ring and with the low preexponential factor associated with the proposed rearrangement of the same (a result of multiple bond rupture and formation). The reactant molecule infrequently accesses this geometry via the random motion of the ligands on the TTIP. Hence the preexponential factor, which is a measure of the frequency at which the low energy activated complex is accessed, is small relative to the typical frequencies associated with molecular vibrations ($\sim 10^{13}$ s⁻¹).

IV. CONCLUSIONS

The CVD of TiO₂ using TTIP has been investigated in a new UHV CVD/thin film characterization facility in order to determine the reaction mechanism and understand the effect of surface structure on the mechanism. The results show that on a single crystal rutile(100) surface there are parallel reactions to deposit TiO₂: reaction (1) forming propene and water as gas phase products and reaction (2) forming propene and isopropanol. Reaction (1) is favored at higher temperatures (650–800 K) where lower surface coverages of adsorbed isopropoxide ligands favor dehydration, whereas at lower temperatures (550–650 K) the proximity of isopropoxide ligands on the adsorbed TTIP favor a concerted elimination to form propene and isopropanol. At high temperatures (>800 K), the rapid reaction rate forms surface defects which aid in the dehydrogenation of the isopropoxide ligands

to form acetone, a process which is more facile on defected polycrystalline surfaces.¹⁶ Thus the single crystal influences which reactions are facile.

ACKNOWLEDGMENTS

The authors would like to thank Samuel Chen and Gustavo Paz-Pujalt of Eastman Kodak Company for useful discussions. Support by the Center for Interfacial Engineering (CIE), a National Science Foundation Engineering Research Center.

- ¹N. Rauche and E. P. Bulte, *J. Electrochem. Soc.* **140**, 145 (1993).
- ²T. Fuyuki and H. Matsunami, *Jpn. J. Appl. Phys.* **25**, 1288 (1986).
- ³H. K. Pulker, G. Paesold, and E. Ritter, *Appl. Opt.* **15**, 2986 (1976).
- ⁴K. S. Yeung and Y. W. Lam, *Thin Solid Films* **109**, 169 (1983).
- ⁵T.-K. Won, S.-G. Yoon, and H.-G. Kim, *J. Electrochem. Soc.* **139**, 3284 (1992).
- ⁶K. L. Siefert and G. L. Griffin, *J. Electrochem. Soc.* **137**, 814 (1990).
- ⁷S. Chen *et al.*, *J. Vac. Sci. Technol. A* **11**, 2419 (1993).
- ⁸S. Chen *et al.* in *Evolution of Surface and Thin Film Microstructure*, edited by H. A. Atwater, E. Chason, M. Grabow, M. Lagally (Materials Research Society, Pittsburgh, PA, 1994), Vol. 280, p. 173.
- ⁹C. A. Muryn, P. J. Hardman, J. J. Crouch, G. N. Raiker, G. Thornton, and D. S.-L. Law, *Surf. Sci.* **251/252**, 747 (1991).
- ¹⁰G. S. Rohrer, V. E. Henrich, and D. A. Bonnell, *Surf. Sci.* **278**, 146 (1992).
- ¹¹R. W. G. Wyckoff, *Crystal Structures*, 2nd ed. (Interscience, New York, 1958), Vol. 1, pp. 250–252.
- ¹²Y. W. Chung, W. J. Lo, and G. A. Somojai, *Surf. Sci.* **64**, 588 (1977).
- ¹³The TTIP was adsorbed at 343 K to prevent multilayer adsorption. Other TPRS experiments showed that when the TTIP was adsorbed onto the substrate at 193 K, a multilayer of TTIP adsorbs, which desorbs to leave a monolayer below 373 K.
- ¹⁴P. Malet and G. Munuera, *J. Chem. Soc. Faraday Trans.* **85**, 4157 (1989).
- ¹⁵P. A. Redhead, *Vacuum* **12**, 203 (1962).
- ¹⁶Y.-M. Wu, D. C. Bradley, and R. M. Nix, *Appl. Surf. Sci.* **64**, 21 (1993).
- ¹⁷T. Kanai, H. Komiyama, and H. Inoue, *Kagaku Kogaku Ronbunshu* **11**, 317 (1985).
- ¹⁸I. Carrizosa and G. Munuera, *J. Catal.* **49**, 174 (1977).
- ¹⁹I. Carrizosa and G. Munuera, *J. Catal.* **49**, 189 (1977).
- ²⁰S. J. Gentry, R. Rudham, and K. P. Wagstaff, *J. Chem. Soc. Faraday Trans. 1* **71**, 657 (1975).
- ²¹M. Nandi, D. Rhubright, and A. Sen, *Inorg. Chem.* **29**, 3065 (1990).
- ²²K. S. Kim and M. A. Barteau, *J. Mol. Catal.* **63**, 103 (1990).